Critical role of RAGE and HMGB1 in inflammatory heart disease

Anna Bangert[a,1], Martin Andrassy[a,1], Anna-Maria Müller[a], Mariella Bockstahler[a], Andrea Fischer[a], Christian H. Volz[a], Christoph Leib[a], Stefan Göser[a], Sevil Korkmaz-Icöz[b], Stefan Zittrich[c], Andreas Jungmann[a], Felix Lasitschka[d], Gabriele Pfitzer[c], Oliver J. Müller[a,e], Hugo A. Katus[a,e], and Ziya Kaya[a,e,2]

[a]Department of Internal Medicine III, University of Heidelberg, 69120 Heidelberg, Germany; [b]Department of Cardiac Surgery, University of Heidelberg, 69120 Heidelberg, Germany; [c]Institute of Vegetative Physiology, University of Cologne, 50931 Cologne, Germany; [d]Institute of Pathology, University of Heidelberg, 69120 Heidelberg, Germany; and [e]DZHK (German Centre for Cardiovascular Research), Partner Site Heidelberg/Mannheim, University of Heidelberg, 69120 Heidelberg, Germany

Edited by Michael T. Lotze, University of Pittsburgh Cancer Institute, Pittsburgh, PA, and accepted by the Editorial Board November 30, 2015 (received for review November 12, 2015)

Autoimmune response to cardiac troponin I (TnI) induces inflammation and fibrosis in the myocardium. High-mobility group box 1 (HMGB1) is a multifunctional protein that exerts proinflammatory activity by mainly binding to receptor for advanced glycation end products (RAGE). The involvement of the HMGB1–RAGE axis in the pathogenesis of inflammatory cardiomyopathy is yet not fully understood. Using the well-established model of TnI-induced experimental autoimmune myocarditis (EAM), we demonstrated that both local and systemic HMGB1 protein expression was elevated in wild-type (wt) mice after TnI immunization. Additionally, pharmacological inhibition of HMGB1 using glycyrrhizin or anti-HMGB1 antibody reduced inflammation in hearts of TnI-immunized wt mice. Furthermore, RAGE knockout (RAGE-ko) mice immunized with TnI showed no structural or physiological signs of cardiac impairment. Moreover, cardiac overexpression of HMGB1 using adeno-associated virus (AAV) vectors induced inflammation in the hearts of both wt and RAGE-ko mice. Finally, patients with myocarditis displayed increased local and systemic HMGB1 and soluble RAGE (sRAGE) expression. Together, our study highlights that HMGB1 and its main receptor, RAGE, appear to be crucial factors in the pathogenesis of TnI-induced EAM, because inhibition of HMGB1 and ablation of RAGE suppressed inflammation in the heart. Moreover, the proinflammatory effect of HMGB1 is not necessarily dependent on RAGE only. Other receptors of HMGB1 such as Toll-like receptors (TLRs) may also be involved in disease pathogenesis. These findings could be confirmed by the clinical relevance of HMGB1 and sRAGE. Therefore, blockage of one of these molecules might represent a novel therapeutic strategy in the treatment of autoimmune myocarditis and inflammatory cardiomyopathy.

myocarditis | cytokines | AAV

Inflammatory cardiomyopathy is a relatively common cause of acute heart failure in the young, for which an efficient and specific therapy is lacking. Although most patients recover completely, some present a deteriorating course. Recent work from our laboratory and others has focused on the dysregulation of the immune system as an essential modulator of disease induction and progression in heart failure (1, 2). In this context, release of cardiac troponin I (TnI) from damaged cardiomyocytes into the circulation is believed to trigger an autoimmune response to TnI (3, 4).

Our group has established an animal model in which immunization with murine cardiac TnI induces severe myocardial inflammation and fibrosis, followed by severe heart failure (1). However, the exact pathomechanism and immune modulators involved in this inflammatory process are not yet fully elucidated.

Extensive work has cast light on the role of high-mobility group box 1 (HMGB1) in the pathogenesis of infectious and noninfectious inflammatory diseases. HMGB1, first described as a DNA binding protein, has subsequently been associated with various pathological conditions such as cardiovascular disease (5, 6), cancer (7), and ischemia/reperfusion (I/R) injury (5). It is a key modulator of innate immune responses and regulates in part adaptive immunity (8). In response to cellular stress, HMGB1 acts as a damage-associated molecular pattern (DAMP) signal after passive release into the extracellular milieu during cell death or active secretion by mononuclear and other cell types (7). It binds to receptors such as receptor for advanced glycation end products (RAGE) and Toll-like receptors (TLRs) such as TLR-2 and -4, leading to the expression of inflammatory cytokines, chemokines, and corresponding receptors (9).

Some studies describe differential effects of HMGB1- or RAGE-dependent signaling with regard to their concentration and release in a particular model or mode of application (10, 11). In a rodent model of myocardial infarction, exogenously administered HMGB1 had a beneficial effect on postinfarct myocardial remodeling (10). Kitahara and colleagues demonstrated reduced necrosis and smaller infarct size after myocardial infarction in transgenic mice overexpressing HMGB1 (12). However, in a murine model of I/R injury, our group recently showed that treatment of wild-type (wt) mice with recombinant HMGB1 increased the infarct size (6). In the same model of I/R injury,

Significance

Myocardial inflammation leads in many cases to cardiomyopathy and contributes to progressive heart failure. The exact pathological mechanism of disease induction and progression in the setting of heart failure is unknown. High-mobility group box 1 (HMGB1), an evolutionarily abundant and highly conserved protein, promotes cardiac inflammation, and in turn immunity, as a damage-associated molecular pattern. HMGB1 stimulates immunity, at least in part, through interaction with its principal binding partner RAGE (receptor for advanced glycation end products). Here we show that HMGB1 and RAGE appear to be important components in cardiac troponin I-induced experimental autoimmune myocarditis as well as in patients with myocarditis. Both molecules represent potential drug targets and show significant potential in heart failure treatment.

Author contributions: A.B., M.A., C.H.V., O.J.M., and Z.K. designed research; A.B., A.-M.M., M.B., A.F., S.G., S.K.-I., A.J., F.L., G.P., and Z.K. performed research; S.K.-I., S.Z., A.J., F.L., G.P., and O.J.M. contributed new reagents/analytic tools; A.B., M.A., A.-M.M., M.B., A.F., C.H.V., C.L., S.G., S.Z., O.J.M., H.A.K., and Z.K. analyzed data; and A.B., M.A., A.-M.M., M.B., A.F., C.H.V., C.L., O.J.M., H.A.K., and Z.K. wrote the paper.

The authors declare no conflict of interest.

This article is a PNAS Direct Submission. M.T.L. is a guest editor invited by the Editorial Board.

Freely available online through the PNAS open access option.

[1]A.B. and M.A. contributed equally to this work.

[2]To whom correspondence should be addressed. Email: ziya.kaya@med.uni-heidelberg.de.

This article contains supporting information online at www.pnas.org/lookup/suppl/doi:10.1073/pnas.1522288113/-/DCSupplemental.

RAGE-deficient mice demonstrated significantly reduced myocardial damage compared with wt mice (6).

The effect of HMGB1 and RAGE on the pathogenesis of cardiac disorders is not only described in preclinical animal models but is also investigated in human cardiac disorders. Different studies have revealed an elevated HMGB1 level in patients with heart failure correlating with disease severity (13–17). In addition to this, some studies have identified RAGE as a prognostic factor in human heart failure (16, 18, 19).

In the present study, we aimed to clarify the role of HMGB1 and RAGE in an experimental model of murine autoimmune myocarditis. This experimental approach enables a reproducible sterile cardiac inflammation, as described previously (1, 20). Furthermore, the clinical relevance of both proteins should be investigated.

Hence, we first studied the expression kinetics of HMGB1 in the inflamed myocardium and serum of wt mice. Then, inhibition of HMGB1 by glycyrrhizin (GL) was performed and heart tissue was analyzed in TnI-induced experimental autoimmune myocarditis (EAM) of wt mice. Additionally, RAGE knockout (RAGE-ko) mice were immunized with TnI to further study the role of RAGE signaling in this EAM model. Finally, the role of the HMGB1–RAGE axis in our model was analyzed by an adeno-associated virus (AAV)9-mediated cardiac overexpression of HMGB1. In a last step, we studied the clinical relevance of HMGB1 and RAGE in patients with myocarditis.

Results

TnI Immunization Induced Myocardial Inflammation and Fibrosis, Increased Myocardial HMGB1 Protein Expression, and Impaired Cardiac Function. First, an EAM was induced in mice (Fig. S1). TnI immunization led to sustained myocardial inflammation and fibrosis, as evidenced by hematoxylin and eosin (HE) and Masson's trichrome (MT) staining and evaluated as grade of inflammation/fibrosis, respectively [HE: TnI, day (d)21: 1.9 ± 0.35; d90: 2 ± 0.5; d270: 2.3 ± 0.4; MT: TnI, d21: 1.2 ± 0.5; d90: 2.3 ± 0.5; d270: 2.3 ± 0.4]. Control buffer-immunized group (CFA) showed neither inflamed nor fibrotic tissue (Fig. 1 *A* and *B*).

Furthermore, TnI immunization up-regulated myocardial HMGB1 protein expression on days 21, 90, and 270, as evaluated by quantitative analysis of immunohistochemical data. In heart tissues of CFA-immunized mice, no myocardial HMGB1 protein could be detected (Fig. 1 *A* and *B*).

Western blot analysis showed a significantly increased myocardial HMGB1 protein level in TnI-immunized mice compared with the CFA-treated group (Fig. 1*C*).

The HMGB1 protein level in serum was also increased in TnI-immunized mice compared with CFA groups over a period of 270 d [TnI, d21: 36.4 ± 5.4 ng/mL; d90: 47.2 ± 11.3 ng/mL; d270: 32.0 ± 5.6 ng/mL vs. CFA, d21: 19.3 ± 5.4 ng/mL, $P < 0.05$; d90: 17.5 ± 1.7 ng/mL, $P < 0.01$; d270: 19.6 ± 9.9 ng/mL, not significant (ns); Fig. 1*D*].

TnI Immunization Activated Specific Signaling Pathways. Signal transducer and activator of transcription (STAT) 3 and c-Jun N-terminal kinase (JNK) were analyzed by Western blot. Significantly increased levels of phosphorylated (p) compared with total (t) protein were detectable for STAT3 and JNK in the early phase of inflammation (day 21) in the hearts of TnI-immunized mice. At later stages of disease (>day 90), p-STAT3 and p-JNK levels were

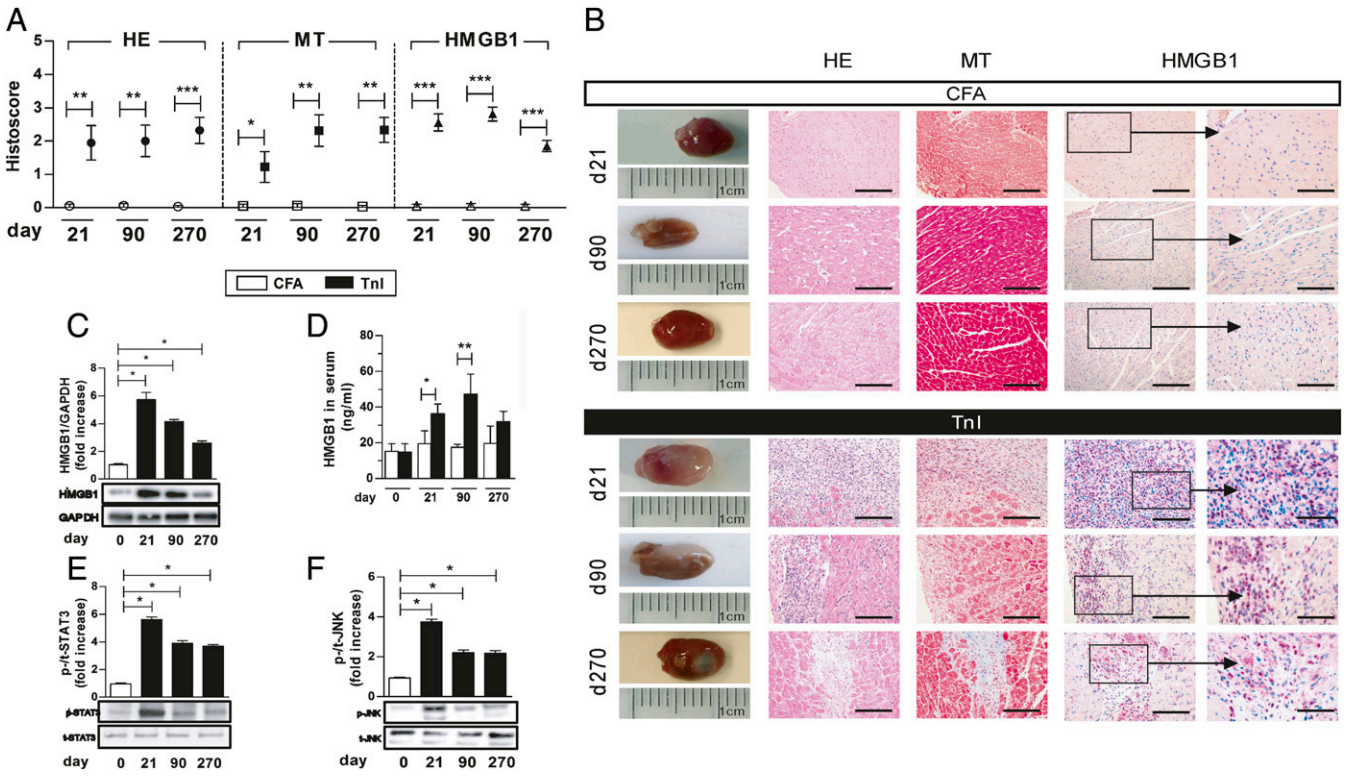

Fig. 1. TnI immunization increased HMGB1 protein level and activated specific signal transduction pathways in myocardium of wt mice. (*A*) Myocardial histoscore of CFA- or TnI-immunized mice for inflammation (HE), fibrosis (MT), and HMGB1 expression on days 21, 90, and 270. (*B*) Corresponding macroscopic pictures (*Left*) and histopathological examinations (*Right*) of immunized mice. [Scale bars, 100 μm (columns 2–4) and 25 μm (column 5).] (*C*) Immunoblot and fold increase of HMGB1 compared with glyceraldehyde-3-phosphate dehydrogenase (GAPDH) in cardiac proteins of TnI-immunized mice on days 0, 21, 90, and 270. (*D*) Serum HMGB1 level in immunized mice. (*E* and *F*) Immunoblot and fold increase of p-STAT3 compared with t-STAT3 (*E*) and p-JNK compared with t-JNK (*F*) in cardiac proteins of TnI-immunized mice on days 0, 21, 90, and 270. Error bars indicate mean ± SEM. $^*P < 0.05$, $^{**}P < 0.01$, $^{***}P < 0.005$.

decreased but still significantly increased compared with CFA-immunized mice (Fig. 1 *E* and *F*).

HMGB1 Inhibition Decreased TnI-Induced Myocardial Inflammation. To study the preventive and therapeutic effect of the HMGB1 inhibition by glycyrrhizin, mice were treated with glycyrrhizin before (GL) and starting with day 14 (GL14) after TnI immunization.

TnI-immunized mice treated with glycyrrhizin displayed improved ejection fraction (EF) as well as significantly reduced high-sensitive troponin T (hs-TnT) levels and myocardial inflammation compared with TnI-immunized and PBS-treated animals in both GL and GL14 groups (hs-TnT: PBS/TnI: 308.0 ± 20.6 pg/mL vs. GL: 105.0 ± 12.6 pg/mL, $P < 0.05$, and vs. GL14: 82.2 ± 22.5 pg/mL, $P < 0.005$; EF: PBS/TnI: 82.3 ± 1.7% vs. GL: 93.5 ± 2.7%, $P < 0.05$, and vs. GL14: 83.2 ± 1.4%, ns; inflammation score: PBS/TnI: 2.8 ± 0.2 vs. GL: 1.2 ± 0.5, $P < 0.05$, and vs. GL14: 0.8 ± 0.5, $P < 0.05$; Fig. 2 *A*–*C*).

HMGB1 inhibition was also analyzed by the administration of anti-HMGB1 antibody (Ab-HMGB1) as well as control antibody (Ab-Cont.) to TnI-immunized mice. Immunized mice treated with Ab-HMGB1 showed a reduced hs-TnT level and inflammation as well as an improved EF compared with Ab-Cont.–treated mice (hs-TnT: Ab-Cont.: 257.5 ± 91.5 pg/mL vs. Ab-HMGB1: 48.9 ± 22.4 pg/mL, $P < 0.1$; EF: Ab-Cont.: 79.8 ± 2.9% vs. Ab-HMGB1: 84.0 ± 1.0%, $P < 0.1$; inflammation score: Ab-Cont.: 1.6 ± 0.5 vs. Ab-HMGB1: 0.9 ± 0.3, $P < 0.05$; Fig. 2 *D*–*F*).

RAGE-Knockout Mice Were Protected from Developing TnI-Induced EAM. The hs-TnT concentration of untreated mice at day 0 was <100 pg/mL (detection limit). In TnI-immunized wt mice, serum levels of hs-TnT were significantly elevated compared with CFA-treated mice (wt/TnI: 312.7 ± 56.1 pg/mL vs. wt/CFA: 124.0 ± 10.2 pg/mL, $P < 0.01$). However, serum concentration levels of hs-TnT in TnI- and CFA-immunized RAGE-ko mice displayed no significant increase compared with untreated mice (Fig. 3*A*).

Furthermore, TnI-immunized RAGE-ko mice showed no pathological alterations in EF in contrast to TnI-immunized wt mice on day 21 (EF: wt/TnI: 74.1 ± 2.2% vs. RAGE-ko/TnI: 87.2 ± 0.7%, $P < 0.001$; Fig. 3*B*).

Myocardial inflammation and fibrosis were almost absent in RAGE-ko mice on day 21 (inflammation score: wt/TnI: 1.9 ± 0.3 vs. RAGE-ko/TnI: 0.2 ± 0.1, $P < 0.005$; fibrosis score: wt/TnI: 1.7 ± 0.3 vs. RAGE-ko/TnI: 0.2 ± 0.1, $P < 0.01$; Fig. 3 *C* and *D*).

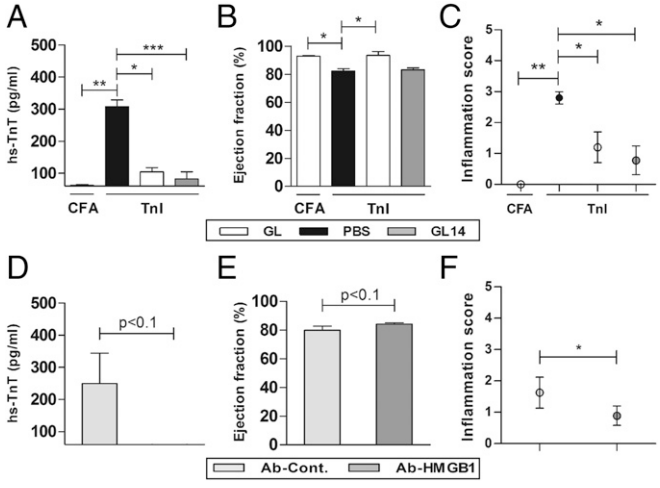

Fig. 2. HMGB1 inhibition decreased TnI-induced myocardial inflammation. Mice were immunized with CFA or TnI and treated daily (GL21) or from day 14 to 21 (GL14) with glycyrrhizin. (*A*) hs-TnT levels in serum of immunized mice treated with glycyrrhizin or control buffer (PBS). (*B*) Ejection fraction. (*C*) Myocardial inflammation score was determined using HE staining on day 21. (*D*) hs-TnT levels in serum of immunized mice treated with anti-HMGB1 antibody or control antibody. (*E*) Ejection fraction. (*F*) Histoscore of inflammation was determined using HE staining on day 21. Error bars indicate mean ± SEM. **P* < 0.05, ***P* < 0.01, ****P* < 0.005.

RAGE Deficiency Resulted in Down-Regulation of Myocardial Transcription Levels of Inflammatory Mediators and Matrix Metalloproteinases and Affected Signaling Pathways. TnI-immunized RAGE-ko mice showed significantly reduced levels of chemokines such as monocyte chemoattractant protein 1 (MCP-1), regulated upon activation normal T-cell expressed and secreted (RANTES), macrophage inflammatory protein (MIP) 1α and MIP-1β, as well as chemokine (C-C motif) receptors (CCRs) such as CCR1/2/5 compared with TnI-immunized wt mice. Cytokines such as tumor necrosis factor (TNFα) and interleukin 6 (IL-6) as well as matrix metalloproteinase 14 (MMP-14) and tissue inhibitor of metalloproteinase 1 (TIMP-1) also displayed significantly reduced levels compared with TnI-immunized wt mice (Fig. 3*E*).

Next, the activity of STAT3 and Janus kinase 2 (JAK2) on day 21 was analyzed. We observed that RAGE-ko mice showed decreased activation of STAT3/JAK2 signaling compared with wt mice when immunized with TnI. Additionally, extracellular signal-regulated protein kinase (ERK) 1/2 and JNK were analyzed. Higher levels of p-ERK1/2 and p-JNK, normalized to their total protein level, were observed in TnI-immunized wt mice but not in RAGE-ko animals (Fig. 3*F*).

Analysis of nuclear extracts of myocardium from immunized RAGE-ko mice demonstrated a significant decrease in NF-κB DNA binding activity compared with TnI-immunized wt mice (Fig. 3*G*).

AAV9-Mediated HMGB1 Overexpression Induced Cardiac Inflammation and Fibrosis in TnI- and CFA-Immunized Mice Independent of RAGE. As a next step in our study, an AAV9-vector system was used to overexpress myocardial HMGB1 (Fig. S1). We detected increased protein levels of cardiac HMGB1 in both CFA-immunized wt and RAGE-ko mice after HMGB1 treatment but no increase in control vector (AAV-luciferase; Luc)-treated mice (Fig. S2*A*). Furthermore, HMGB1 serum levels were increased in both CFA-immunized wt and RAGE-ko mice after HMGB1 treatment, albeit not significant (Fig. S2*B*).

The hs-TnT levels in CFA-immunized mice without AAV9 treatment were <100 pg/mL (detection limit). HMGB1 treatment and only CFA immunization generated a significant increase in hs-TnT levels (Fig. 4*A*) in both wt and RAGE-ko mice compared with Luc-AAV–treated and CFA-immunized mice (wt/HMGB1/CFA: 448.9 ± 50.5 pg/mL vs. wt/Luc/CFA: 112.0 ± 12.0 pg/mL, $P < 0.005$; RAGE-ko/HMGB1/CFA: 510.0 ± 94.3 pg/mL vs. RAGE-ko/Luc/CFA: 92.0 ± 4.9 pg/mL, $P < 0.05$). Additional TnI immunization did not increase hs-TnT release any further in HMGB1-treated wt or RAGE-ko mice. In contrast, TnI immunization increased hs-TnT release in Luc-AAV–treated wt but not in RAGE-ko mice. Furthermore, cardiac function of the animals was evaluated (Fig. 4*B*). Overexpression of HMGB1 alone without TnI immunization decreased the EF significantly in both wt and RAGE-ko groups. In contrast, Luc-AAV–treated and CFA-immunized mice showed no significant change in cardiac function (wt/HMGB1/CFA: 41.7 ± 9.7% vs. wt/Luc/CFA: 86.9 ± 0.9%, $P < 0.01$; RAGE-ko/HMGB1/CFA: 53.7 ± 9.4% vs. RAGE-ko/Luc/CFA: 86.5 ± 1.0%, $P < 0.005$). Maximal decrease in cardiac EF has been seen in wt mice with cardiac overexpression of HMGB1 and additional immunization with TnI.

Histopathological changes were assessed, and both wt and RAGE-ko mice treated with HMGB1 and CFA immunization showed significant inflammation and fibrosis in the myocardium

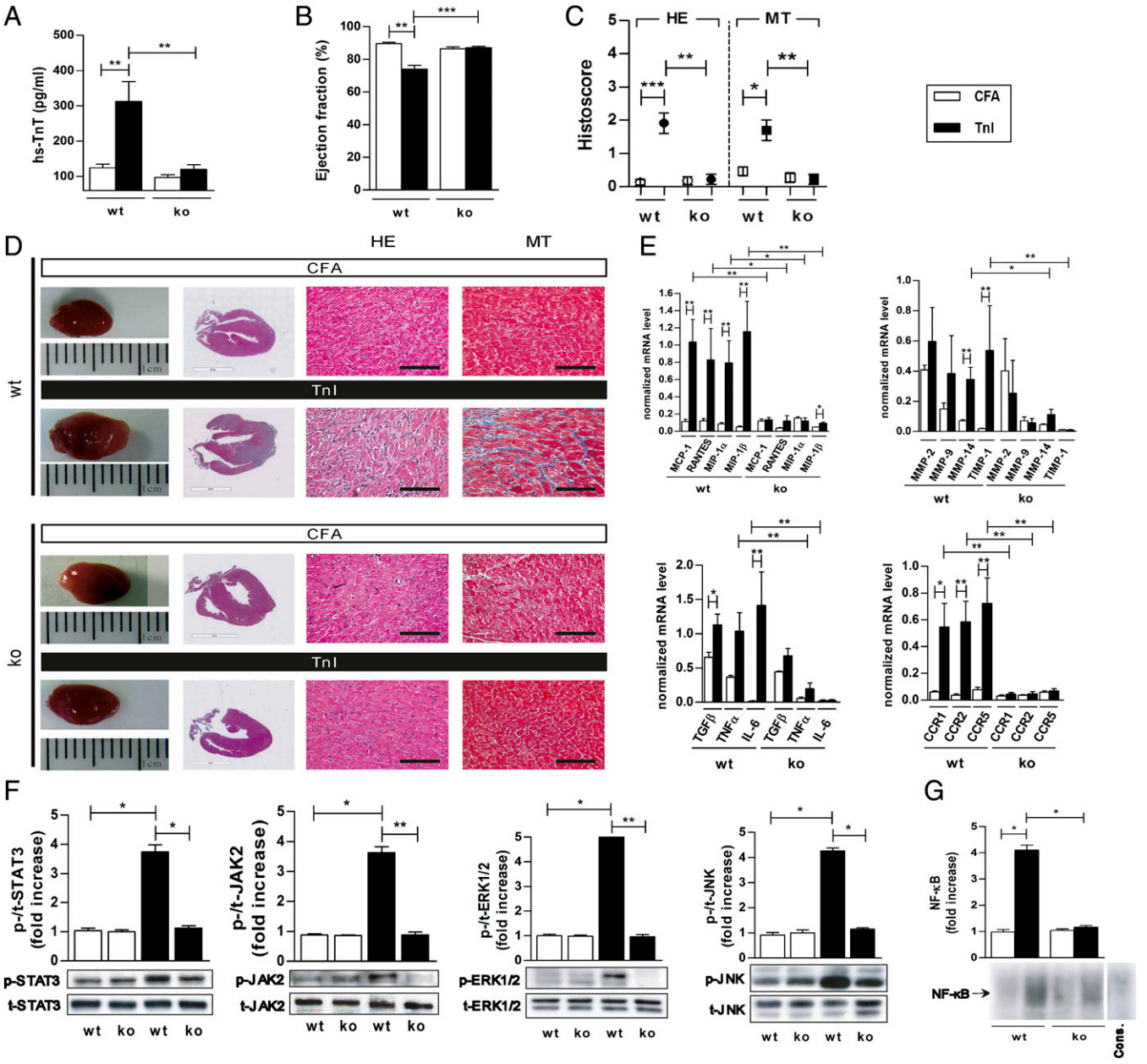

Fig. 3. RAGE-ko mice were protected from developing TnI-induced EAM. Wt and RAGE-ko mice were immunized with CFA or TnI. Measurements were done on day 21. (*A*) hs-TnT levels in serum of immunized mice. (*B*) Ejection fraction. (*C*) Histoscore of inflammation and fibrosis in the hearts of immunized mice. (*D*) Representative macroscopic pictures (*Left*) and histopathological examinations (*Right*) of hearts stained with HE and MT. [Scale bars, 3 mm (column 2) and 100 μm (columns 3 and 4).] (*E*) Myocardial mRNA levels of genes involved in cardiac inflammation. (*F*) Heart tissues were analyzed by Western blot, and fold increase of phosphorylated compared with total STAT3, JAK2, ERK1/2, and JNK proteins was thereby detected. (*G*) Electrophoretic mobility shift assay was performed to measure the NF-κB binding activity in myocardium. Specificity of NF-κB binding activity was shown by including a 160-fold molar excess of unlabeled consensus NF-κB oligonucleotide (Cons.). Fold increase of NF-κB compared to Cons. was calculated. Error bars indicate mean ± SEM. $*P < 0.05$, $**P < 0.01$, $***P < 0.005$.

compared with Luc-AAV–treated mice (inflammation score: wt/HMGB1/CFA: 0.7 ± 0.2 vs. wt/Luc/CFA: 0.1 ± 0.1, $P < 0.01$; RAGE-ko/HMGB1/CFA: 1.5 ± 0.2 vs. RAGE-ko/Luc/CFA: 0.3 ± 0.2, $P < 0.01$; fibrosis score: wt/HMGB1/CFA: 1.9 ± 0.2 vs. wt/Luc/CFA: 0.4 ± 0.2, $P < 0.005$; RAGE-ko/HMGB1/CFA: 2.8 ± 0.5 vs. RAGE-ko/Luc/CFA: 0.8 ± 0.1, $P < 0.01$; Fig. 4 *C* and *D*).

Hence, TnI-immunized RAGE-ko mice showed a significant increase in myocardial inflammation and fibrosis when HMGB1 was overexpressed. However, this effect was lower than in TnI-immunized and HMGB1-treated wt mice. Hearts treated with Luc-AAV and immunized with CFA were almost free from proinflammatory and profibrotic structural changes. Representative macroscopic and microscopic findings of AAV9 vectors (HMGB1 or Luc) and CFA- or TnI-immunized mice are shown in Fig. 4*E*.

HMGB1 overexpression alone without TnI immunization led to cardiac damage, inflammation, fibrosis, and deteriorated cardiac performance. Therefore, all further animal studies were performed in CFA-immunized mice.

Myocardial AAV9-Mediated HMGB1 Overexpression Altered the Transcription of Diverse Immunomodulators, Activated Intracellular Signaling Pathways, and Enhanced NF-κB Binding Activity. HMGB1

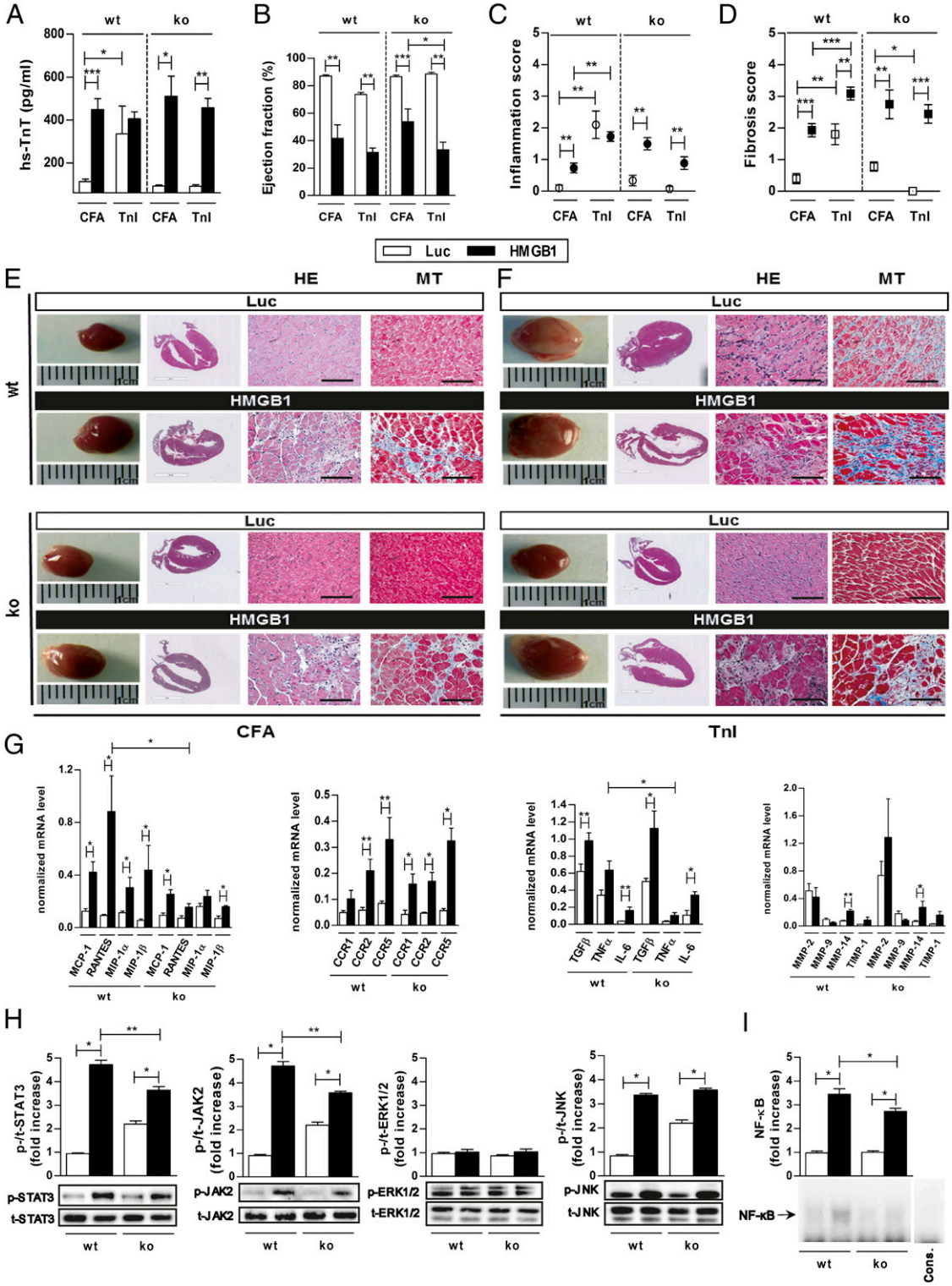

Fig. 4. HMGB1 treatment induced cardiac damage and affected activation of inflammation-related genes and signaling cascades in wt and RAGE-ko mice. Wt and RAGE-ko mice were treated with AAV9-HMGB1 or control vector (Luc) and were immunized with CFA or TnI. Measurements were done on day 21. (*A*) hs-TnT production in serum of immunized mice upon AAV9-vector treatment. (*B*) Ejection fraction. (*C*) Inflammation. (*D*) Fibrosis score. (*E* and *F*) Representative macroscopic pictures (*Left*) and histopathological examinations (*Right*) of hearts stained with HE and MT. [Scale bars, 3 mm (column 2) and 100 μm (columns 3 and 4).] (*G*) Myocardial mRNA levels were analyzed by qPCR. (*H*) Heart tissues were analyzed by Western blot, and fold increase of phosphorylated compared with total STAT3, JAK2, ERK1/2, and JNK proteins was thereby detected. (*I*) Electrophoretic mobility shift assay was performed to measure the NF-κB binding activity in myocardium. Specificity of NF-κB binding activity was shown by including a 160-fold molar excess of unlabeled consensus NF-κB oligonucleotide (Cons.). Fold increase of NFkB compared to Cons. was calculated. Error bars indicate mean ± SEM. $*P < 0.05$, $**P < 0.01$, $***P < 0.005$.

treatment led to increased transcription levels of CCR2 and -5 in wt and RAGE-ko mice compared with Luc-AAV–treated mice. In addition, RANTES and MIP-1α were up-regulated in HMGB1-overexpressed wt but not in RAGE-ko mice. Except for MMP-14, we could not observe any significant alterations in transcription levels of other MMPs in wt and RAGE-ko mice after HMGB1 treatment. Furthermore, RANTES and TNFα were significantly higher in HMGB1-overexpressed wt compared with RAGE-ko animals (Fig. 4*F*).

Western blot analysis further revealed significantly increased protein levels of activated STAT3, JAK2, and JNK in HMGB1-treated groups. The activation of STAT3 and JAK2 in HMGB1-overexpressed RAGE-ko mice was significantly lower compared with the corresponding wt groups. No differences were observed in the protein expression of ERK1/2 (Fig. 4*G*).

Nuclear extracts of the myocardium from HMGB1-treated wt and RAGE-ko mice demonstrated a significant increased NF-κB DNA binding activity compared with Luc-AAV–treated groups. Wt mice showed a stronger NF-κB DNA binding activity than RAGE-ko mice (Fig. 4*H*).

HMGB1 Overexpression Resulted in Up-Regulated Myocardial TLR-2 and -4 Levels in RAGE-Knockout Mice. Our results showed that myocardial HMGB1 overexpression seems to induce an inflammatory immune response independent of RAGE. We next investigated whether TLR-2 or -4 might play a role in the development of HMGB1-induced inflammatory cardiomyopathy. For this, we performed quantitative (q)PCR and Western blot analysis of myocardial tissue post AAV9-vector injection from wt and RAGE-ko mice.

The mRNA expression levels of TLR-2 showed a slight increase in RAGE-ko and a significant increase in wt mice after HMGB1 treatment compared with the Luc-AAV groups. Moreover, up-regulated TLR-4 mRNA levels were demonstrated in HMGB1-overexpressed RAGE-ko compared with wt mice ($P < 0.06$; Fig. S3*A*).

Myocardial protein levels of TLR-2 and -4 were significantly up-regulated in HMGB1-overexpressed wt mice compared with Luc-AAV–treated mice. Furthermore, TLR-2 was significantly increased in wt compared with RAGE-ko mice after HMGB1 treatment (Fig. S3*B*).

HMGB1 Expression Was Elevated in Plasma as Well as Myocardial Biopsies of Patients with Myocarditis. Immunohistochemical myocardial staining of HMGB1 of biopsies of patients with myocarditis demonstrated an increased number of nuclear HMGB1-positive cells in inflamed tissue compared with myocarditis-negative patients (Fig. 5 *A* and *B*). Plasma HMGB1 and soluble RAGE (sRAGE) levels in patients with myocarditis were elevated compared with healthy controls (HMGB1: 24.4 ± 5.8 ng/mL vs. 4.4 ± 0.7 ng/mL, $P < 0.001$; sRAGE: 1020.8 ± 125.8 pg/mL vs. 675.0 ± 56.1 pg/mL, $P < 0.05$; Fig. 5 *C* and *D*).

Discussion

Here we studied the role of HMGB1 and its receptor, RAGE, in the pathogenesis of TnI-induced EAM as a model of inflammatory cardiomyopathy. Our results show that immunization with TnI not only induces severe myocardial inflammation and fibrosis with subsequent heart failure but also leads to an increase in serum and myocardial HMGB1 protein levels. In contrast, cardiac tissue injury could be prevented by administration of glycyrrhizin. Additionally, in RAGE-ko mice, myocardial inflammation and fibrosis were almost completely suppressed, and TnI immunization did not affect cardiac performance. Furthermore, cardiac overexpression of HMGB1 induced inflammation in the hearts of both wt and RAGE-ko mice. This finding suggests that the proinflammatory effect of HMGB1 in our model is not necessarily dependent on RAGE only. Finally, elevated HMGB1 and sRAGE levels in patients with myocarditis compared with healthy controls point out the clinical relevance of this inflammatory pathway.

Myocarditis is defined as inflammation of the myocardium with consequent myocardial injury, often leading to cardiomyopathy. It is the leading cause of heart failure in young patients. The precise pathomechanisms involved in disease induction and progression are not yet fully understood. Medical treatment is mostly based on the patient's symptoms and is not specific for the disease.

Recently, HMGB1 was found to be instrumental in mediating an immune response to tissue damage and infection (9, 21). Our previous work has focused on the role of HMGB1 in various cardiac and metabolic stress models characterizing HMGB1 as an important initiator of inflammation and fibrosis (6, 22, 23).

The functions of HMGB1 are dependent on its localization. Intracellular HMGB1 acts as a regulator of transcription by interacting with chromatin structures of DNA. HMGB1 can be either actively secreted or passively released into the extracellular milieu upon cell death (7). Upon reaching the extracellular environment, HMGB1 acts as a DAMP, activating TLRs and RAGE, which in turn can promote an immune response (24, 25).

In this study, we observed elevated HMGB1 protein levels in both serum and inflamed myocardium upon TnI immunization of EAM mice. Furthermore, we detected an elevated HMGB1 deposition in inflamed myocardial tissue of patients with acute myocarditis compared with biopsies taken from patients without any signs of inflammation as control. Moreover, we measured an elevated HMGB1 level in plasma of patients with myocarditis compared with healthy controls. Accordingly, it can be hypothesized at this point that the elevated HMGB1 levels of mice as well as myocarditis patients were either due to cardiomyocyte damage or actively triggered by immune cells. However, a combination of both is also possible. In fact, it has been reported that HMGB1 can be actively secreted by immune cells, such as monocytes and macrophages, which may be dependent on TLR-4 (26). Due to the fact that macrophages are key regulators in the pathogenesis of myocarditis, it is likely that the elevated HMGB1 level we observed upon TnI immunization may at least be in part triggered by macrophages (26) or activated monocytes (27). The intriguing role of HMGB1 in chronic inflammation and autoimmunity has already been reported in rheumatoid arthritis and systemic lupus erythematosus (8). In line with our findings, HMGB1 levels are up-regulated in blood or other biological fluids (e.g., synovial fluid) and affected tissues in rheumatoid arthritis and systemic lupus erythematosus as well (28). Even in patients with cardiac disorders, an elevated HMGB1 level correlating with disease severity could be detected. This increased HMGB1 level may serve as a diagnostic parameter (13–17).

Previous studies showed the critical role of HMGB1 in JAK/STAT and JNK signaling (6, 29–31) and its potential to induce cardiomyocyte apoptosis by triggering the JNK pathway. In line with these findings, we observed activation of the STAT3 and JNK signaling pathways in our model of TnI-induced EAM.

To study the inflammatory processes of TnI-induced EAM, we further analyzed the inhibition of HMGB1 using the well-established inhibitor glycyrrhizin as well as Ab-HMGB1. Glycyrrhizin inhibits the chemotactic and mitogenic functions of HMGB1 and thereby exerts its antiinflammatory properties (32). Accordingly, we showed that administration of glycyrrhizin as well as anti-HMGB1 antibody reduces myocardial inflammation and attenuates TnI-induced myocarditis. Similarly, cardiac protective effects mediated by HMGB1 inhibition could also be shown in other models, such as I/R injury. This I/R injury study demonstrated that glycyrrhizin decreased the amount of p-JNK (33). Other mitogen-activated protein kinases, such as p38 or ERK1/2, did not appear to be affected (22). Taken together, these data suggest that HMGB1 seems to promote the progression of cardiac inflammation. In contrast to this, Limana et al. showed that local administration of

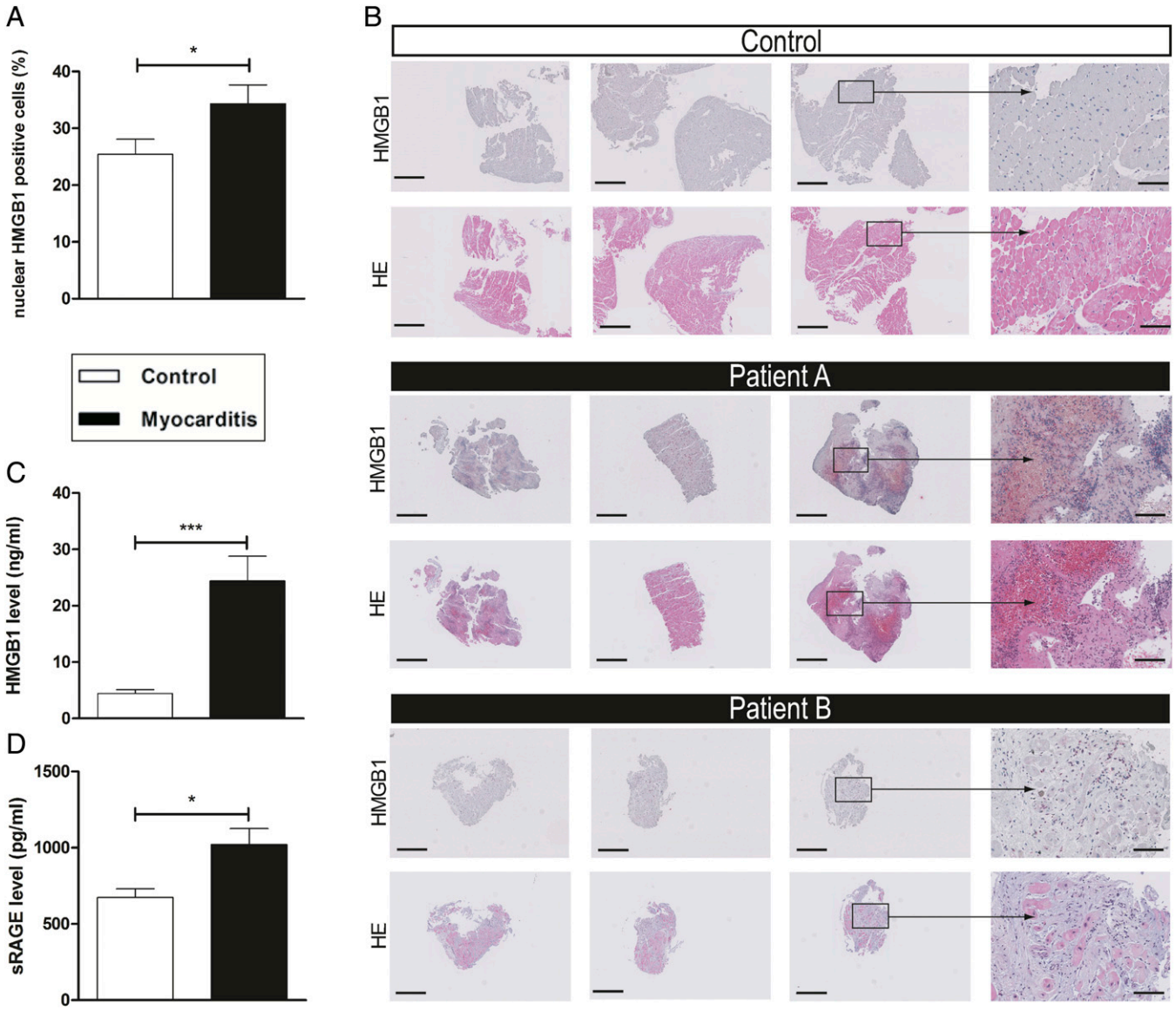

Fig. 5. Myocarditis patients displayed increased myocardial expression of HMGB1 and elevated levels of HMGB1 and sRAGE in plasma. (*A*) The number of nuclear HMGB1-positive cells was increased in the myocardium of patients with myocarditis ($n = 13$) compared with those of the control group ($n = 11$). (*B*) Representative histopathological stainings (HMGB1 and HE) of endomyocardial biopsies (three biopsies for each patient shown). [Scale bars, 500 μm (columns 1–3) and 100 μm (column 4).] (*C* and *D*) Patients with myocarditis ($n = 10$) displayed significantly elevated levels of HMGB1 (*C*) and sRAGE (*D*) in their plasma compared with healthy controls ($n = 11$). Error bars indicate mean ± SEM. $*P < 0.05$, $***P < 0.005$.

low doses of HMGB1 induced an improvement in cardiac function as well as myocardial regeneration after myocardial infarction (10). These controversial data may be ascribed to different experimental setups in the two studies, which is already discussed by Ramasamy et al. (29). Moreover, the type of cell death seems to influence the HMGB1 protein level, which is important for the induction of either cardiac repair or remodeling (30).

In our study, we further investigated the role of RAGE in TnI-induced autoimmune myocarditis. Several studies point out the activation of RAGE by HMGB1 (7, 24). Altered protein levels of RAGE isoforms in patients suffering from heart failure also refer to the clinical relevance of this pathway (16, 18, 19). Therefore, based on the EAM model, our results show for the first time, to our knowledge, that RAGE-ko mice are almost completely protected from developing TnI-induced autoimmune myocarditis. Ablation of RAGE resulted in significantly decreased levels of several inflammatory mediators such as chemokines, chemokine receptors, MMPs, and cytokines, which are important for the pathogenesis of autoimmune myocarditis (20). Additionally, NF-κB binding activity was reduced in immunized RAGE-ko mice.

RAGE-dependent sustained NF-κB activation has been implicated in various chronic inflammatory diseases (34, 35). The downstream effects on regulating transcriptional levels of proinflammatory mediators upon RAGE ligation have been reviewed recently, and our results strongly suggest that the protective effect observed in RAGE-ko mice was due to suppression of RAGE downstream signaling (36). Sirois and colleagues showed that RAGE promotes DNA uptake into endosomes and lowers the immune recognition threshold for the activation of TLR-9, the principal DNA-recognizing transmembrane signaling receptor (37). This potentially can lead to undesirable autoimmune disorders such as systemic lupus erythematosus (38).

Data on the role of the HMGB1–RAGE axis in lymphoid cells, especially in an autoimmune setting, remain scarce. Initial findings were published by Tian et al., who demonstrated a critical role for HMGB1 in RAGE-dependent activation of plasmacytoid dendritic cells and B cells in concert with TLR-9 driving autoimmune processes (39). It has also previously been shown that RAGE deficiency affected maturation and migration of dendritic cells and their cross-talk with natural killer (NK) cells, which is pivotal for sustaining innate immunity and initiating a subsequent adaptive immune response (40, 41). In addition, RAGE deficiency has been linked to drastically reduced T-cell activation and differentiation, leading to suppressed B-cell response (40, 42).

This led to the hypothesis that the blunted immune response in RAGE-ko mice could be caused by inhibited activation of B-cells or reduced inflammatory cell recruitment and chemotaxis. More research needs to be done to identify the exact signaling mechanisms and cells involved in this RAGE-mediated process.

To further analyze the role of HMGB1 signaling in TnI-induced EAM, we overexpressed HMGB1 specifically in the heart using an AAV9-vector system. In AAV9 vectors, the HMGB1 expression cassette is under the control of a cytomegalovirus (CMV)-enhanced 260-bp myosin light chain (MLC)-2v promoter, which ensures cardiomyocyte-specific expression (43, 44). Here we observed myocardial inflammation and fibrosis independent of TnI immunization in both HMGB1-overexpressing wt and in RAGE-ko mice, suggesting that HMGB1 may induce cardiac inflammation by mechanisms independent of RAGE. There were no signs of inflammation in other organs. Our results strongly suggest that the inflammatory response we observed in HMGB1-overexpressing RAGE-ko animals seems to be at least in part triggered by the activation of STAT3, JNK, and JAK2, because we observed elevated levels of those signaling molecules in HMGB1-overexpressing, CFA-immunized RAGE-ko mice. Because the observed proinflammatory effect of HMGB1 was not dependent on RAGE, we assessed whether TLRs might be involved. TLRs as well as RAGE belong to the family of pattern-recognition receptors (PRRs) and are components of innate immunity (7, 24, 25). TLRs are known to be involved in sensing different exogenous foreign molecular products, known as PAMPs (pathogen-associated molecular patterns), whereas RAGE is predominantly involved in the recognition of endogenous molecules (7). Indeed, we observed an up-regulation of TLR-2 and -4 when HMGB1 was overexpressed. In this context, Paulus et al. showed recently that polyethylene particles, which act as a PAMP, induce TLR-2 up-regulation in the synovial layer of mice (45). Furthermore, HMGB1–nucleosome complexes are known to activate the immune response through TLR-2 signaling (46).

Because HMGB1 is known to act as a DAMP when passively released to the extracellular milieu upon tissue injury/destruction, we hypothesize that in our model it up-regulates TLR-2 and -4 either directly by intercalating TLR transcription via its DNA binding capacity or indirectly by affecting cytokine expression levels.

Both HMGB1-treated and CFA-immunized wt and RAGE-ko groups displayed increased mRNA levels of nearly all measured cytokines/chemokines and their receptors. We could not show any significant difference between these groups, and hence TLRs might be responsible for this release. In fact, several studies showed that mainly TLR-4 is required for HMGB1-mediated cytokine production (47). We also detected significantly enhanced RANTES, MCP-1, and MIP-1α mRNA levels in HMGB1-treated wt in comparison with RAGE-ko mice. This may indicate an additional RAGE-, TLR-2–, or other receptor-dependent cytokine activating pathway. In this context, Bianchi et al. showed a RAGE-dependent up-regulation of chemokines, including RANTES and MIP-1α, in microglia (48). Another study showed that an HMGB1–nucleosome complex mediated inflammatory cytokine activation through TLR-2 (46). Because HMGB1 can also bind to other cytokines, such as IL-1β, the inflammatory response can also be mediated through the receptors of partner molecules (7). We further observed a significant difference between wt and RAGE-ko HMGB1-treated mice in TLR-2 protein levels. These effects may indicate an interaction between RAGE and TLR-2. This could be possible due to an interaction between RAGE and a typical TLR adaptor protein, MyD88 (31, 49). Furthermore, this could also indicate the presence of increased HMGB1 immune complexes caused during necrosis, such as HMGB1–DNA (39) mediated by RAGE and HMGB1–nucleosome, which mainly signals through TLR-2 (46).

Moreover, increased TLR-4 protein levels were observed in both HMGB1-treated wt and RAGE-ko mice. These might indicate that the HMGB1 in our study is in a reduced form, which might stimulate TLR-4 and finally results in enhanced cytokine release (24, 47). Additional studies are strongly needed to clearly unravel the role of HMGB1–receptor activity in the pathogenesis of inflammatory cardiomyopathy.

In summary, we showed that there is a significant expression of HMGB1 in the myocardium of TnI-immunized wt mice. This was associated with increased HMGB1 levels in the serum of these mice. Inhibition of HMGB1 resulted in protection of tissue damage in TnI-induced EAM. Furthermore, ablation of RAGE nearly abolished TnI-induced myocardial inflammation/fibrosis and consecutive heart failure. This protective effect might be associated with impaired activation of NF-κB and decreased mRNA expression levels of inflammatory cytokines, chemokines, and chemokine receptors. In addition, our study demonstrates that myocardial overexpression of HMGB1 alone seems to be able to induce myocardial inflammation independent of RAGE. HMGB1 and sRAGE seem to play an important role also in patients with acute myocarditis, because we demonstrated elevated HMGB1 and sRAGE levels in plasma and increased expression of HMGB1 in myocardial biopsies of patients suffering from acute myocarditis.

Additional studies are necessary to further investigate the exact pathomechanism of these findings. Our study provides valuable information on the role of HMGB1 and RAGE in the pathogenesis of myocardial inflammation. Targeting the HMGB1–RAGE axis might be a promising novel tool for the treatment of inflammatory cardiomyopathy.

Materials and Methods

Mice. Female A/J wild-type mice were obtained from Envigo. RAGE-ko mice were backcrossed to the A/J background for at least six generations (50). All mice were maintained in the animal facility unit of the University of Heidelberg. In all experiments, 5- to 6-wk-old female mice were used. The Animal Care and Use Committee of the University of Heidelberg approved all procedures involving the use and care of animals (German Animal Protection Code G-142/09).

Preparation of Recombinant Murine Cardiac Troponin I. The expression of murine cardiac troponin subunit I was performed via *Escherichia coli* and purified as described previously (51). In addition to purification via ion-exchange chromatography, TnI was applied to a cardiac troponin C affinity column as a second purification step (52). TnI-containing fractions were dialyzed against 1 mmol/L HCl, and then lyophilized and stored at −80 °C.

Immunization with TnI. All mice were treated with an s.c. injection of 100 μL emulsion, which contained either 150 μg murine cardiac TnI in supplemented complete Freund's adjuvant with 5 mg/mL *Mycobacterium tuberculosis* H37Ra (Sigma) or 1× PBS control buffer in adjuvant alone. We named these control buffer-immunized groups "CFA."

Glycyrrhizin Treatment. Glycyrrhizin (10 mg/kg; Sigma) was administered daily by i.p. injection, from day 0 to 21 or from day 14 to 21, in addition to TnI or CFA immunization (days 0 and 7). Mice were killed on day 21. Buffer solution (1× PBS) was used as control. The dose of glycyrrhizin was chosen on the basis of our pilot studies.

Anti-HMGB1 Antibody Treatment. Ab-HMGB1 (anti-HMGB1 antibody 2G7) was kindly provided by Kevin Tracey, The Feinstein Institute for Medical Research, Manhasset, NY. As a control antibody, mouse IgG2b-κ (Sigma) was used. The wt mice were treated i.p. with 50 μg antibody every second day for 3 wk in addition to the TnI immunization (days 0 and 7) and were killed on day 21.

Plasmid Construction and AAV9 Vector. Gene synthesis of a codon-optimized murine HMGB1 sequence (National Center for Biotechnology Information reference no. AAH64790.1) was performed by GeneArt. At the 5′ end a restriction site for BamHI and a Kozak sequence were added, whereas at the 3′ end a restriction site for BsrGI was introduced. The cDNA of Renilla luciferase was amplified from the plasmid pGL4 from Promega with primers carrying a BamHI site at the 5′ end and a BsrGI site at the 3′ end. Both cDNAs were inserted using BamH1/BsrGI sites into the vector genome plasmid pdsCMV-MLC260-EGFP (44), resulting in pdsCMV-MLC260-HMGB1 (AAV9-HMGB1; HMGB1) and pdsCMV-MLC260-luciferase (AAV9-luciferase; Luc). Self-complementary AAV9 vectors were generated by cotransfection of the respective genome plasmids with pDP9rs, a derivate from pDP2rs (53) with the AAV9 cap gene from p5E18-VD2-9. Vectors were purified as described before (43, 44).

Experimental Setup. The experimental setup for all groups is summarized in Fig. S1 and Table S1.

i) Wt mice were immunized with either TnI or CFA on days 0, 7, 60, and 245 and killed on day 21, 90, or 270, as described previously (1).
ii) HMGB1 inhibition was analyzed in immunized wt mice by using glycyrrhizin over a period of 21 d (TnI/GL) and for a therapeutic approach from day 14 to 21 (TnI/GL14). Immunization with TnI or CFA was done on days 0 and 7 and mice were killed on day 21.

Furthermore, HMGB1 inhibition was analyzed in immunized wt mice treated with Ab-HMGB1 or Ab-Cont. Immunization with TnI was performed on days 0 and 7 and mice were killed on day 21.

iii) Wt or RAGE-ko mice were immunized with either TnI or CFA on days 0 and 7 and killed on day 21.
iv) Wt or RAGE-ko mice received a systemic single dose of 0.5–1.0 × 10^{12} AAV9-HMGB1 vector or AAV9-luciferase vector by i.v. injection via the tail vein 2 wk before (day −14) the initial TnI immunization on day 0. A second immunization was performed on day 7. Thirty-five days post AAV9-vector transfer, all mice were killed for further analysis.

Determination of hs-TnT, HMGB1, and sRAGE Serum/Plasma Protein Levels. hs-TnT assay was used as an indicator for myocardial damage in serum of mice 21 d after treatment with either TnI or CFA. Collected serum samples were diluted (1:20) with cold 0.9% NaCl solution. The hs-TnT was measured by the electrochemiluminescence method (ECLIA; Elecsys 2010 analyzer). Details of the test principle have been described before (54).

For a quantitative determination of HMGB1 protein in serum/plasma, a high-sensitivity sandwich ELISA (Shino-Test) was performed according to the manufacturer's instructions (55). ELISA for detection of sRAGE levels (BioVendor) in plasma was performed according to the manufacturer's instructions.

Histopathology and Immunohistochemistry. Mice were killed by cervical dislocation and all hearts were removed, fixed in formalin [10% (vol/vol)], and subsequently embedded in paraffin. Sections of 3- to 5-μm thickness were cut and stained with hematoxylin and eosin to determine the level of inflammation. Additionally, Masson's trichrome staining was performed to detect collagen deposition to assess the grade of fibrosis. Five sections of each heart were inspected in a double-blinded manner by two independent investigators by light microscopy to evaluate inflammation and fibrosis.

Immunohistochemical HMGB1 staining of murine and human heart sections was performed with rabbit polyclonal anti-HMGB1 antibody as the primary reagent (1:250; Abcam) and biotinylated donkey anti-rabbit antibody (1:200; Dianova) as the secondary reagent. An avidin-biotin-alkaline phosphatase system (ABC-AP; Dako) was used according to the manufacturer's instructions. Parallel incubations with nonimmune IgGs of the relevant species served as negative control.

HE-, MT-, and HMGB1-stained sections were analyzed as described in Table S2. To quantify the HMGB1 expression in human heart sections, TMARKER software was used as previously described (56).

Quantitative PCR. An RNeasy Mini Kit (Qiagen) was used according to the manufacturer's instructions to isolate total RNA from hearts. One microgram RNA was used to synthesize cDNA (iScript cDNA Synthesis Kit; Bio-Rad). Quantitative PCR was then performed using 25 ng cDNA in a 20-μL reaction volume. A denaturation step at 95 °C for 5 min was carried out, followed by 40 cycles of denaturation at 95 °C for 10 s and annealing at 60 °C for 30 s. The primer sequences are listed in Table S3. Quantification was done by using a QuantiFast SYBR Green PCR Kit (Qiagen) according to the manufacturer's instructions and using an iCycler iQ2 Detection System (Bio-Rad). The measured gene expressions were normalized to the expression of the reference gene L32.

Echocardiography. Echocardiographic measurements of the first experimental approach (*i*) were performed with an ATL HDI 9000 (Philips) ultrasonograph with a 10-MHz annular array transducer as previously described (1).

In experimental approaches (*ii*), (*iii*), and (*iv*), echocardiography was performed using a VisualSonics Vevo 2100 System, 30-MHz linear MicroScan transducer (MSH400), especially optimized for cardiovascular experiments in mice. Parasternal long-axis projection cine loops were acquired at the level of clear visible walls of the aortic annulus. Furthermore, parasternal short-axis cine loops were performed at the level of the papillary muscles. Stored data of the B-mode and M-mode images were executed and analyzed by a single operator using a proprietary software package provided with the Vevo 2100 platform. The presented percentage ejection fraction was measured in the long axis and calculated using formulas of the Cardiac Measurement Package (Vevo 2100 1.5.0). Echocardiography was conducted in a blinded manner.

Western Blotting. For Western blot analysis, flash-frozen heart tissues were ground in RIPA buffer (0.1% SDS, 1.0% Triton X-100, 0.1% sodium deoxycholate, 140 mM NaCl) supplemented with Halt Protease and Phosphatase Inhibitor Cocktail (Life Technologies). The tissue suspension was passed three times through a 25G needle to lyse the membrane. The tubes were centrifuged at 18,000 × g for 15 min. The supernatant was used for the determination of protein concentration using Protein Assay Bradford Reagent (Bio-Rad).

Twenty micrograms of total myocardial protein extract per lane was separated on NuPAGE Bis-Tris gels (Invitrogen) and transferred to a polyvinylidene fluoride (PVDF) transfer membrane (Immobilon-P; Millipore). The membrane was first blocked [5% (wt/vol) bovine serum albumin/Tris-buffered saline] for 1 h at room temperature (RT) and then incubated with a primary antibody for 1 h at RT (Table S4). After repeated washing steps, the blots were incubated with secondary antibody (horseradish peroxidase-coupled anti-rabbit IgG, 1:3,000) for 1 h at RT. Protein bands were detected using a chemiluminescence agent (GE Healthcare). Quantitative analysis was performed with ImageJ software (NIH). GAPDH served as a loading control.

Electrophoretic Mobility Shift Assay. The binding activity of p65-NF-κB in nuclear protein extracts (70 μg) of heart tissue was assayed with ^{32}P radioactively labeled oligonucleotide sequences (5′-AGT TGA GGG GAC TTT CCC AGG C-3′) at 50,000 cpm by autoradiography. The experiment is based on electrophoretic mobility of a protein–nucleic acid complex, which migrates more slowly than the corresponding free nucleic acid, and was performed as previously described (57).

Human Samples. Endomyocardial biopsies from patients with myocarditis according to the Dallas criteria were used for staining (HMGB1 and HE). In addition, blood samples were taken for HMGB1 and sRAGE detection. Biopsies taken from patients with no signs of inflammation and blood samples from healthy donors served as controls.

The study was conducted in accordance with the Declaration of Helsinki and was approved by the local ethics committee of the University of Heidelberg. All subjects included in the study provided written informed consent.

Statistical Analysis. Results are expressed as mean ± SEM. Data were analyzed using the Mann–Whitney *U* and two-way ANOVA tests. Values of $P < 0.05$ were considered statistically significant and are marked as $^{*}P < 0.05$, $^{**}P < 0.01$, $^{***}P < 0.005$.

ACKNOWLEDGMENTS. The authors acknowledge Dr. Angelika Bierhaus and her collaborators for sharing the RAGE-ko mice, Dr. Kevin Tracey (The Feinstein Institute for Medical Research) for kindly providing the anti-HMGB1 antibody, and Dr. Tanja Weis as well as Dr. Alamara Karimi for providing the human plasma samples. We thank Kirsten Keilbach, Renate Öttl, Vesna Vukovic, Karl Varadi, Patrick Heger, and Annette Buttler for technical assistance, and David Stanmore for critically reading the manuscript. This work was supported by the Deutsche Forschungsgemeinschaft

Research Grants AN 403/2-1 (to Z.K. and M.A.), in part KA 1797/7-1 (to Z.K.) and the Sonderforschungsbereich 612 (to G.P.). Furthermore, the DZHK (German Centre for Cardiovascular Research) and the BMBF (German Ministry of Education and Research) (Z.K. and O.M.) partly supported this work.

1. Göser S, et al. (2006) Cardiac troponin I but not cardiac troponin T induces severe autoimmune inflammation in the myocardium. *Circulation* 114(16):1693–1702.
2. Kaya Z, et al. (2001) Contribution of the innate immune system to autoimmune myocarditis: A role for complement. *Nat Immunol* 2(8):739–745.
3. Eriksson S, Halenius H, Pulkki K, Hellman J, Pettersson K (2005) Negative interference in cardiac troponin I immunoassays by circulating troponin autoantibodies. *Clin Chem* 51(5):839–847.
4. Leuschner F, et al. (2008) Absence of auto-antibodies against cardiac troponin I predicts improvement of left ventricular function after acute myocardial infarction. *Eur Heart J* 29(16):1949–1955.
5. Oozawa S, et al. (2008) Effects of HMGB1 on ischemia-reperfusion injury in the rat heart. *Circ J* 72(7):1178–1184.
6. Andrassy M, et al. (2008) High-mobility group box-1 in ischemia-reperfusion injury of the heart. *Circulation* 117(25):3216–3226.
7. Sims GP, Rowe DC, Rietdijk ST, Herbst R, Coyle AJ (2010) HMGB1 and RAGE in inflammation and cancer. *Annu Rev Immunol* 28:367–388.
8. Andersson U, Tracey KJ (2011) HMGB1 is a therapeutic target for sterile inflammation and infection. *Annu Rev Immunol* 29:139–162.
9. Lotze MT, Tracey KJ (2005) High-mobility group box 1 protein (HMGB1): Nuclear weapon in the immune arsenal. *Nat Rev Immunol* 5(4):331–342.
10. Limana F, et al. (2005) Exogenous high-mobility group box 1 protein induces myocardial regeneration after infarction via enhanced cardiac C-kit+ cell proliferation and differentiation. *Circ Res* 97(8):e73–e83.
11. Rossini A, et al. (2008) HMGB1-stimulated human primary cardiac fibroblasts exert a paracrine action on human and murine cardiac stem cells. *J Mol Cell Cardiol* 44(4): 683–693.
12. Kitahara T, et al. (2008) High-mobility group box 1 restores cardiac function after myocardial infarction in transgenic mice. *Cardiovasc Res* 80(1):40–46.
13. Kohno T, et al. (2009) Role of high-mobility group box 1 protein in post-infarction healing process and left ventricular remodelling. *Cardiovasc Res* 81(3):565–573.
14. Liu T, et al. (2015) Increased serum HMGB1 level may predict the fatal outcomes in patients with chronic heart failure. *Int J Cardiol* 184:318–320.
15. Volz HC, et al. (2012) HMGB1 is an independent predictor of death and heart transplantation in heart failure. *Clin Res Cardiol* 101(6):427–435.
16. Wang LJ, et al. (2011) Increased serum high-mobility group box-1 and cleaved receptor for advanced glycation endproducts levels and decreased endogenous secretory receptor for advanced glycation endproducts levels in diabetic and non-diabetic patients with heart failure. *Eur J Heart Fail* 13(4):440–449.
17. Yan XX, et al. (2009) Increased serum HMGB1 level is associated with coronary artery disease in nondiabetic and type 2 diabetic patients. *Atherosclerosis* 205(2):544–548.
18. Lu L, et al. (2009) Increased glycated albumin and decreased esRAGE levels are related to angiographic severity and extent of coronary artery disease in patients with type 2 diabetes. *Atherosclerosis* 206(2):540–545.
19. Koyama Y, et al. (2008) Soluble receptor for advanced glycation end products (RAGE) is a prognostic factor for heart failure. *J Card Fail* 14(2):133–139.
20. Kaya Z, et al. (2008) Identification of cardiac troponin I sequence motifs leading to heart failure by induction of myocardial inflammation and fibrosis. *Circulation* 118(20):2063–2072.
21. Bianchi ME (2007) DAMPs, PAMPs and alarmins: All we need to know about danger. *J Leukoc Biol* 81(1):1–5.
22. Volz HC, Kaya Z, Katus HA, Andrassy M (2010) The role of HMGB1/RAGE in inflammatory cardiomyopathy. *Semin Thromb Hemost* 36(2):185–194.
23. Andrassy M, et al. (2011) HMGB1 as a predictor of infarct transmurality and functional recovery in patients with myocardial infarction. *J Intern Med* 270(3):245–253.
24. Harris HE, Andersson U, Pisetsky DS (2012) HMGB1: A multifunctional alarmin driving autoimmune and inflammatory disease. *Nat Rev Rheumatol* 8(4):195–202.
25. Yang H, Tracey KJ (2010) Targeting HMGB1 in inflammation. *Biochim Biophys Acta* 1799(1-2):149–156.
26. Wang F, et al. (2010) Fas (CD95) induces rapid, TLR4/IRAK4-dependent release of proinflammatory HMGB1 from macrophages. *J Inflamm (Lond)* 7:30.
27. Gardella S, et al. (2002) The nuclear protein HMGB1 is secreted by monocytes via a non-classical, vesicle-mediated secretory pathway. *EMBO Rep* 3(10):995–1001.
28. Magna M, Pisetsky DS (2014) The role of HMGB1 in the pathogenesis of inflammatory and autoimmune diseases. *Mol Med* 20:138–146.
29. Ramasamy R, Yan SF, Schmidt AM (2008) Stopping the primal RAGE reaction in myocardial infarction: Capturing adaptive responses to heal the heart? *Circulation* 117(25):3165–3167.
30. Vogel S, et al. (2015) Necrotic cell-derived high mobility group box 1 attracts antigen-presenting cells but inhibits hepatocyte growth factor-mediated tropism of mesenchymal stem cells for apoptotic cell death. *Cell Death Differ* 22(7):1219–1230.
31. Rojas A, et al. (2013) The receptor for advanced glycation end-products: A complex signaling scenario for a promiscuous receptor. *Cell Signal* 25(3):609–614.
32. Mollica L, et al. (2007) Glycyrrhizin binds to high-mobility group box 1 protein and inhibits its cytokine activities. *Chem Biol* 14(4):431–441.
33. Zhai CL, et al. (2012) Glycyrrhizin protects rat heart against ischemia-reperfusion injury through blockade of HMGB1-dependent phospho-JNK/Bax pathway. *Acta Pharmacol Sin* 33(12):1477–1487.
34. Bierhaus A, et al. (2004) Loss of pain perception in diabetes is dependent on a receptor of the immunoglobulin superfamily. *J Clin Invest* 114(12):1741–1751.
35. Schmidt AM, Yan SD, Yan SF, Stern DM (2001) The multiligand receptor RAGE as a progression factor amplifying immune and inflammatory responses. *J Clin Invest* 108(7):949–955.
36. van Zoelen MA, Achouiti A, van der Poll T (2011) RAGE during infectious diseases. *Front Biosci (Schol Ed)* 3:1119–1132.
37. Belinsky GS, et al. (2014) Patch-clamp recordings and calcium imaging followed by single-cell PCR reveal the developmental profile of 13 genes in iPSC-derived human neurons. *Stem Cell Res (Amst)* 12(1):101–118.
38. Horton CG, Pan ZJ, Farris AD (2010) Targeting Toll-like receptors for treatment of SLE. *Mediators Inflamm* 2010:498980.
39. Tian J, et al. (2007) Toll-like receptor 9-dependent activation by DNA-containing immune complexes is mediated by HMGB1 and RAGE. *Nat Immunol* 8(5):487–496.
40. Dumitriu IE, et al. (2005) Release of high mobility group box 1 by dendritic cells controls T cell activation via the receptor for advanced glycation end products. *J Immunol* 174(12):7506–7515.
41. Semino C, Angelini G, Poggi A, Rubartelli A (2005) NK/iDC interaction results in IL-18 secretion by DCs at the synaptic cleft followed by NK cell activation and release of the DC maturation factor HMGB1. *Blood* 106(2):609–616.
42. Chen Y, et al. (2008) RAGE ligation affects T cell activation and controls T cell differentiation. *J Immunol* 181(6):4272–4278.
43. Müller OJ, et al. (2006) Improved cardiac gene transfer by transcriptional and transductional targeting of adeno-associated viral vectors. *Cardiovasc Res* 70(1):70–78.
44. Müller OJ, Schinkel S, Kleinschmidt JA, Katus HA, Bekeredjian R (2008) Augmentation of AAV-mediated cardiac gene transfer after systemic administration in adult rats. *Gene Ther* 15(23):1558–1565.
45. Paulus AC, et al. (2014) Polyethylene wear particles induce TLR 2 upregulation in the synovial layer of mice. *J Mater Sci Mater Med* 25(2):507–513.
46. Urbonaviciute V, et al. (2008) Induction of inflammatory and immune responses by HMGB1-nucleosome complexes: Implications for the pathogenesis of SLE. *J Exp Med* 205(13):3007–3018.
47. Yang H, et al. (2010) A critical cysteine is required for HMGB1 binding to Toll-like receptor 4 and activation of macrophage cytokine release. *Proc Natl Acad Sci USA* 107(26):11942–11947.
48. Bianchi R, Kastrisianaki E, Giambanco I, Donato R (2011) S100B protein stimulates microglia migration via RAGE-dependent up-regulation of chemokine expression and release. *J Biol Chem* 286(9):7214–7226.
49. Sakaguchi M, et al. (2011) TIRAP, an adaptor protein for TLR2/4, transduces a signal from RAGE phosphorylated upon ligand binding. *PLoS One* 6(8):e23132.
50. Bierhaus A, et al. (2001) Diabetes-associated sustained activation of the transcription factor nuclear factor-kappaB. *Diabetes* 50(12):2792–2808.
51. Krüger M, Pfitzer G, Stehle R (2003) Expression and purification of human cardiac troponin subunits and their functional incorporation into isolated cardiac mouse myofibrils. *J Chromatogr B Analyt Technol Biomed Life Sci* 786(1-2):287–296.
52. al-Hillawi E, Minchin SD, Trayer IP (1994) Overexpression of human cardiac troponin-I and troponin-C in *Escherichia coli* and their purification and characterisation. Two point mutations allow high-level expression of troponin-I. *Eur J Biochem* 225(3):1195–1201.
53. Grimm D, Kay MA, Kleinschmidt JA (2003) Helper virus-free, optically controllable, and two-plasmid-based production of adeno-associated virus vectors of serotypes 1 to 6. *Mol Ther* 7(6):839–850.
54. Andrassy M, et al. (2012) HMGB1 is associated with atherosclerotic plaque composition and burden in patients with stable coronary artery disease. *PLoS One* 7(12): e52081.
55. Yamada S, Yakabe K, Ishii J, Imaizumi H, Maruyama I (2006) New high mobility group box 1 assay system. *Clin Chim Acta* 372(1-2):173–178.
56. Schüffler PJ, et al. (2013) TMARKER: A free software toolkit for histopathological cell counting and staining estimation. *J Pathol Inform* 4(Suppl):S2.
57. Andrassy M, et al. (2006) Posttranslationally modified proteins as mediators of sustained intestinal inflammation. *Am J Pathol* 169(4):1223–1237.